Supporting Information for

Controlling the Circadian Clock with High Temporal Resolution through Photodosing

Dušan Kolarski[1], Akiko Sugiyama[2], Ghislain Breton[3], Christin Rakers[4], Daisuke Ono[5], Albert Schulte[1], Florence Tama[2,6,7], Kenichiro Itami[2], Wiktor Szymanski[1,8], Tsuyoshi Hirota[2,*], and Ben L. Feringa[1,*]

[1] Centre for Systems Chemistry, Stratingh Institute for Chemistry, University of Groningen, Nijenborgh 4, 9747 AG, Groningen, The Netherlands

[2] Institute of Transformative Bio-Molecules (WPI-ITbM), Nagoya University, Chikusa, Nagoya 464-8601, Japan

[3] Department of Integrative Biology and Pharmacology, McGovern Medical School, University of Texas Health Science Center at Houston, 6431 Fannin St, MSB 4.216, 77030 Houston, US

[4] Graduate School of Pharmaceutical Sciences, Kyoto University, 46-29 Yoshida-shimoadachi-cho, Sakyo-ku, Kyoto 606-8501, Japan

[5] Department of Neuroscience II, Research Institute of Environmental Medicine, Nagoya University, Furo-cho, Chikusa-ku, Nagoya 464-8601, Japan

[6] Department of Physics, Graduate School of Science, Nagoya University, Nagoya, Japan

[7] Computational Structural Biology Unit, RIKEN-Center for Computational Science, Kobe, Hyogo 650-0047, Japan

[8] University Medical Center Groningen, Department of Radiology, Medical Imaging Center, University of Groningen, Hanzeplein 1, 9713 GZ Groningen, The Netherlands

*Correspondence: b.l.feringa@rug.nl (B.L.F.), thirota@itbm.nagoya-u.ac.jp (T.H.)

KEY REAGENTS, RESOURCES TABLE

REAGENT or RESOURCE	SOURCE	IDENTIFIER
Chemicals, Peptides, and Recombinant Proteins		
Bovine Serum Albumin	Sigma	Cat# A2153-50G
DL-Dithiothreitol	TCI	Cat# D3647
TRIS HCl	Acros	Cat# 228030010
ATP	Fisher Scientific	Cat# R0441
CSNK1A1	Invitrogen	Cat# PV3850
RRKDLHDDEEDEAMSITA	AnaSpec	Cat# 60547-1
CSNK1D1	Merck Milipore	Cat# 14-520
RKKKAEpSVASLTSQCSYSS	AnaSpec	Custom made
X1PSG	GIBCO	Cat# 10378-016
Penicillin, streptomycin, L-glutamine	Nacalai Tesque	Cat# 06168-34
Luciferin	PROMEGA	Cat# E1603
DMEM	Gibco	Cat# 12800-017
Fetal bovine serum	Equitech-Bio	Cat# SFBM30
DMEM	Sigma	Cat# D2902-10X1L
B-27 Supplement	Gibco	Cat# 17504001
HEPES	Nacalai Tesque	Cat# 17557-94
Sodium bicarbonate	Wako Pure Chemical	Cat# 195-16411
D-Luciferin	Gold Biotechnology	Cat# LUCK
DMEM	Gibco	Cat# 12100-046
Fetal bovine serum	Sigma	Cat#:172012
D-Luciferin Potassium Salt	Wako Pure Chemical	Cat# 12605116
Experimental Models: Organisms/Strains		
Human: *Bmal1-dLuc* U2OS cells	Hirota et al., 2008	N/A
Mouse: *Per2::Luc* knockin	Yoo et al., 2004	N/A
Software and Algorithms		
MultiCycle	Actimetrics	N/A
ClockLab	Actimetrics	N/A
Kronos	Atto	N/A
Prism	GraphPad Software	N/A
Clustal Omega 2.1	EMBL-EBI	https://www.ebi.ac.uk/Tools/msa/clustalo/
Schrödinger's LigPrep, Glide	Small-Molecule Drug Discovery Suite 2017-4, Schrödinger, LLC, New York, NY	https://www.schrodinger.com/
Statsmodel python library	Seabold, 2010	https://www.statsmodels.org/stable/index.html#
Python	Python Software Foundation	http://www.python.org

EXPERIMENTAL MODEL AND SUBJECT DETAILS

Cell Line

Bmal1-dLuc U2OS cells were maintained as described previously.[1]

Tissue explant

All mouse studies were approved by the Animal Experiment Committee of Nagoya University and performed in accordance with guidelines. *Per2::Luc* knockin mice[2] were obtained from Dr. Joseph S. Takahashi.

Zebrafish

Zebrafish *Danio rerio* strains were maintained under accordance with approved institutional protocols at the McGovern Medical School at the University of Texas Health Science Center Houston. All experiments using zebrafish were approved by IACUC protocol AWC-13-124. Transgenic per3:luc line (g1Tg/+(AB)) (RRID:ZIRC_ZL1167)[3] was acquired from Zirc.

METHODS DETAILS

General reagent information

Preparation of commercially unavailable compounds: unless stated otherwise, all reactions were carried out in oven- and flame-dried glassware using standard Schlenk techniques and were run under nitrogen atmosphere. The reaction progress was monitored by TLC. Starting materials, reagents and solvents were purchased from Sigma–Aldrich, Acros, Fluka, Fischer, TCI, J.T. Baker or Macron and were used as received, unless stated otherwise. Solvents for the reactions were of quality puriss., p.a.. Anhydrous solvents were purified by passage through solvent purification column (MBraun SPS-800). For aqueous solutions, deionized water was used.

General considerations

Thin Layer Chromatography analyses were performed on commercial Kieselgel 60, F254 silica gel plates with fluorescence-indicator UV254 (Merck, TLC silica gel 60 F254). For detection of components, UV light at λ = 254 nm or λ = 365 nm was used. Alternatively, oxidative staining using aqueous basic potassium permanganate solution ($KMnO_4$) or aqueous acidic cerium phosphomolybdic acid solution (Seebach's stain) was used. Drying of solutions was performed with $MgSO_4$ and volatiles were removed with a rotary evaporator (Büchi, R-300).

General analytical information

Nuclear Magnetic Resonance spectra were measured with an Agilent Technologies 400-MR (400/54 Premium Shielded) spectrometer (400 MHz). All spectra were measured at room temperature (22–24 °C). Chemical shifts for the specific NMR spectra were reported relative to the residual solvent peak [in ppm; $CDCl_3$: δ_H = 7.26; $CDCl_3$: δ_C = 77.16; *d*$_6$-DMSO: δ_H = 2.50; *d*$_6$-DMSO: δ_C = 39.52]. The multiplicities of the signals are denoted by s (singlet), d (doublet), t (triplet), q (quartet), hept (heptet), m (multiplet), br (broad signal). All ^{13}C-NMR spectra are ^{1}H-broadband decoupled.

High-resolution mass spectrometric measurements were performed using a Thermo scientific LTQ OrbitrapXL spectrometer with ESI ionization.

Melting points were recorded using a Stuart analogue capillary melting point SMP11 apparatus.

All the reactions were performed in CEM Discover SP-D microwave reactor. Room temperature UV-Vis absorption spectra were recorded on an Agilent 8453 UV-Visible Spectrophotometer using Uvasol grade solvents. UPLC-MS measurements were done using ThermoFischer Scientific Vanquish UPLC System on C18 column.

Irradiation experiments were performed with UV lamp (Spectroline, ENB-280C/FE, 1x8 Watt or SLUV-6, AS ONE), LED system (3 x 1000 mW, λ_{max} = 400 nm, FWHM 11.9 nm, Sahlmann Photochemical Solutions), and custom-built (Prizmatix/Mountain Photonics) multi-wavelength fiber coupled LED-system (FC6-LED-WL) using 365A LED.

Chemical synthesis

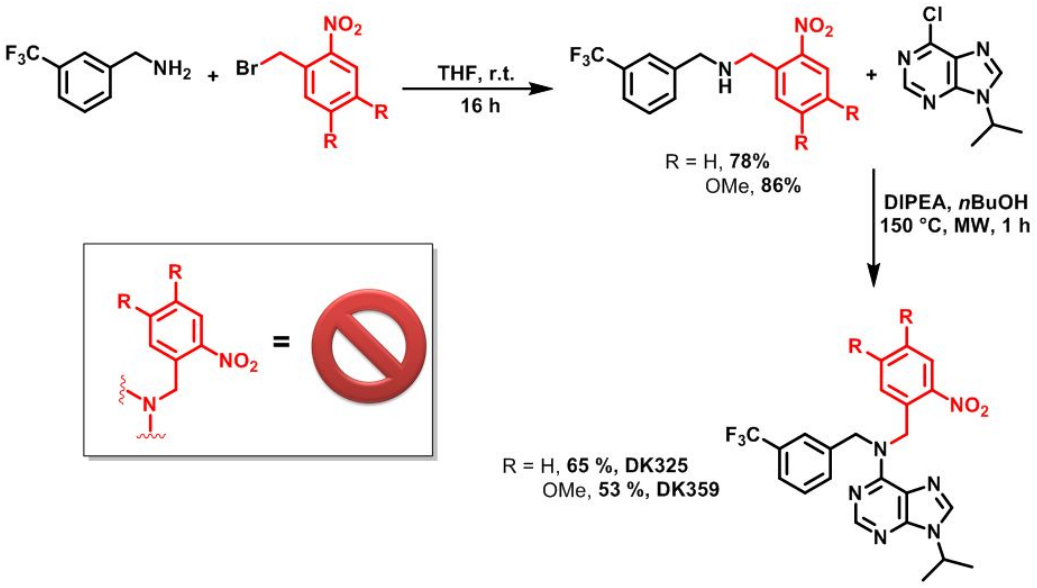

Scheme 1. Synthetic scheme for DK325 and DK359.

N-(2-nitrobenzyl)-1-(3-(trifluoromethyl)phenyl)methanamine

A solution of 3-(trifluoromethyl)benzylamine (0.81 g, 4.6 mmol, 2.0 equiv) and 4,5-dimethoxy-2-nitrobenzyl bromide (0.50 g, 2.3 mmol, 1.0 equiv) in THF (5.0 ml) was stirred at room temperature overnight. A precipitate was removed by filtration and the solvent was removed under reduced pressure. The product was purified by flash column chromatography (SiO_2, PhMe/EtOAc 6:1) to give N-(4,5-dimethoxy-2-nitrobenzyl)-1-(3-(trifluoromethyl)phenyl)methanamine (0.46 g, 1.5 mmol, 64%) as the yellow oil.

^{1}H NMR (400 MHz, $CDCl_3$) δ 7.96 (d, *J* = 7.8 Hz, 1H), 7.64 – 7.53 (m, 4H), 7.52 (d, *J* = 8.0 Hz, 1H), 7.47 – 7.41 (m, 2H), 4.08 (s, 2H), 3.90 (s, 2H), 2.20 (s, 3H); ^{13}C NMR (101 MHz, $CDCl_3$) δ 149.20, 140.13, 134.45, 133.23, 131.60 (d, *J* = 1.4 Hz), 131.56, 130.78 (d, *J* = 31.9 Hz), 128.65 (d, *J* = 56.8 Hz), 125.46, 125.10 – 124.83 (m), 124.88, 124.15 (q, *J* = 3.7 Hz), 122.75, 52.75, 50.09; ^{19}F NMR (376 MHz, $CDCl_3$) δ -62.60; FTIR $\tilde{\nu}$ 3350, 3069, 2846, 1610, 1524, 1447, 1325, 1160, 1117, 1071, 857, 788, 701, 661, 506 cm^{-1}; HRMS (ESI$^+$) calc. for $C_{15}H_{13}N_2F_3O_2H$ $[M+H]^+$: 311.1002, found: 311.0998.

N-(4,5-dimethoxy-2-nitrobenzyl)-1-(3-(trifluoromethyl)phenyl)methanamine

A solution of 3-(trifluoromethyl)benzylamine (3.1 g, 18 mmol, 2.2 equiv) and 4,5-dimethoxy-2-nitrobenzyl bromide (2.2 g, 8.0 mmol, 1.0 equiv) in THF (30 ml) was stirred at room temperature overnight. A precipitate was removed by filtration and the solvent was removed under reduced pressure. The product was purified by flash column chromatography (SiO_2, PhMe/EtOAc 6:1) to give N-(4,5-dimethoxy-2-nitrobenzyl)-1-(3-(trifluoromethyl)phenyl)methanamine (1.9 g, 5.0 mmol, 63%) as the yellow oil.

^{1}H NMR (400 MHz, $CDCl_3$) δ 7.65 (s, 1H), 7.62 (s, 1H), 7.54 (d, *J* = 7.7 Hz, 1H), 7.50 (d, *J* = 8.1 Hz, 1H), 7.43 (t, *J* = 7.7 Hz, 1H), 7.04 (s, 1H), 4.05 (s, 2H), 3.94 (s, 3H), 3.92 (s, 3H), 3.89 (s, 2H); ^{19}F NMR (376 MHz, $CDCl_3$) δ -62.58; ^{13}C NMR (101 MHz, $CDCl_3$) δ 153.24, 147.75, 141.03 (d, *J* = 7.7 Hz), 131.41 (d, *J* = 1.4 Hz), 130.72, 130.70 (d, *J* = 32.1 Hz), 128.85, 125.52, 124.69 (q, *J* = 3.8 Hz), 123.90 (q, *J* = 3.8 Hz), 122.82, 112.55, 108.23, 56.3, 56.27, 52.77, 50.63; FTIR $\tilde{\nu}$ 3352, 2938, 2848, 1614, 1579, 1515, 1453, 1268, 1160, 1060, 987, 870, 794, 702, 659 cm^{-1}; HRMS (ESI$^+$) calc. for $C_{17}H_{17}N_2F_3O_4H$ [M+H]$^+$: 371.1213, found: 371.1207.

9-isopropyl-N-(2-nitrobenzyl)-N-(3-(trifluoromethyl)benzyl)-9H-purin-6-amine (DK325)

The reaction was carried out using a microwave vessel (10 ml) equipped with a magnetic stirring bar, in the presence of air. 6-Chloro-9-isopropyl-*9H*-purine (Boucherle et al., 2014) (0.12 g, 0.62 mmol, 1.0 equiv), N-(2-nitrobenzyl)-1-(3-(trifluoromethyl)phenyl)methanamine (0.25 g, 0.81 mmol, 1.3 equiv), DIPEA (0.54 ml, 3.1 mmol, 5.0 equiv) and *n*-BuOH (6.0 mL) were added in sequence. The resulting mixture was reacted under microwave irradiation (200 W) at 150 °C for 45 min. After the reaction was finished (followed by TLC), the solvent was removed under reduced pressure and the product was purified by flash column chromatography (SiO_2, PhMe/EtOAc 95:5 → 9:1) to give DK325 (0.19 mg, 0.42 mmol, 67%) as the yellow oil that solidifies upon cooling.

^{1}H NMR (400 MHz, $CDCl_3$) δ 8.40 (s, 1H), 8.06 (dd, *J* = 8.1, 1.3 Hz, 1H), 7.78 (s, 1H), 7.56 – 7.43 (m, 5H), 7.43 – 7.34 (m, 3H), 7.27 – 7.22 (m, 1H), 7.18 – 7.14 (m, 0H), 4.87 (hept, *J* = 6.8 Hz, 1H), 1.60 (d, *J* = 6.8 Hz, 7H). ^{13}C NMR (101 MHz, $CDCl_3$) δ 154.72, 152.14, 150.87, 148.59, 138.55, 136.87, 133.54, 131.41, 131.19 – 130.71 (m), 130.44 (d), 129.13, 128.27, 127.82, 125.33, 125.23, 124.60 (q, *J* = 3.7 Hz), 124.34 (q, *J* = 3.7 Hz), 122.62, 51.48, 49.03, 46.87, 22.61. ^{19}F NMR (376 MHz, $CDCl_3$) δ -62.52; FTIR $\tilde{\nu}$ 2979, 1773, 1580, 1524, 1473, 1447, 1327, 1195, 1120, 1072, 980, 792, 649 cm^{-1}; HRMS (ESI$^+$) calc. for $C_{23}H_{21}N_6F_3O_2H$ [M+H]$^+$: 471.1750, found: 471.1750.

N-(4,5-dimethoxy-2-nitrobenzyl)-9-isopropyl-N-(3-(trifluoromethyl)benzyl)-9H-purin-6-amine (DK359)

The reaction was carried out using a microwave vessel (30 ml) equipped with a magnetic stirring bar, in the presence of air. 6-Chloro-9-isopropyl-9H-purine (Boucherle et al., 2014) (50 mg, 0.26 mmol, 1.0 equiv), N-(4,5-dimethoxy-2-nitrobenzyl)-1-(3-(trifluoromethyl)phenyl)methanamine (0.13 g, 0.36 mmol, 1.4 equiv), DIPEA (0.23 mL,1.3 mmol, 5.0 equiv) and *n*-BuOH (2.5 ml) were added in sequence. The resulting mixture was reacted under microwave irradiation (200 W) at 150 °C for 45 min. After the reaction was finished (followed by TLC), the solvent was removed under reduced pressure and the product was purified by flash column chromatography (SiO_2, PhMe/EtOAc 95:5 → 9:1) to give DK359 (56 mg, 0.12 mmol, 47%) as the yellow oil that solidifies upon cooling.

^{1}H NMR (400 MHz, $CDCl_3$) δ 8.43 (s, 1H), 7.80 (s, 1H), 7.68 (s, 1H), 7.54 (s, 1H), 7.51 (d, *J* = 7.5 Hz, 1H), 7.46 (d, *J* = 7.7 Hz, 1H), 7.40 (t, *J* = 7.7 Hz, 1H), 6.75 (s, 1H), 5.64 (s, 2H), 5.40 (s, 2H), 4.90 (hept, *J* = 6.8 Hz, 1H), 3.92 (s, 3H), 3.67 (s, 3H), 1.61 (d, *J* = 6.8 Hz, 6H). FTIR $\tilde{\nu}$ 2971, 1584, 1516, 1326, 1272, 1218, 1163, 1058, 980, 929, 869, 794, 652 cm^{-1}; HRMS (ESI$^+$) calc. for $C_{25}H_{25}N_6F_3O_4H$ [M+H]$^+$: 531.1962, found: 531.1957.

Docking simulation

Multiple sequence alignments for casein kinase isoforms (Uniprot IDs: Q9HCP0, Q9Y6M4, P78368, P48729, P48730, P49674) were performed using the EMBL-EBI webservice Clustal 2.1.[4–6] Three-dimensional structures of molecules Longdaysin, DK325, and DK359 were generated from SMILES via the standardized ligand preparation protocol (LigPrep) implemented in the Schrödinger suite (Small-Molecule Drug Discovery Suite 2017-4, Schrödinger, LLC, New York, NY, 2017). X-ray crystal structures of proteins CK1α [PDB entry 5FQD][7]

and CK1δ [PDB entries 4KBK,[8] 4TN6 (chain A (ligand-bound) and chain B (apo)), 4TWC[9]] were subjected to protein preparation procedures including the addition of hydrogens, reconstruction of missing residues, adjustment of protonation states to pH 7, and minimization of the protein structures with convergence of heavy atoms to an RMSD of 0.3 Å using force field OPLS3.[10] Molecular docking simulations were executed using Glide in XP precision mode.[11–13] Statistical significance of differences in estimated ligand binding energies was evaluated using one-way ANOVA and Tukey's post hoc analysis via python (Python Software Foundation. Python Language Reference, version 2.7. Available at http://www.python.org) and the statsmodel package.[14]

Photo-deprotection studies

The process of photo-deprotection of DK325 and DK359 was followed by UPLC-MS (ThermoFischer Scientific Vanquish UPLC System; C18 column: Acquity UPLC HSS T3 1.8 µm, 2.1 × 150 mm; eluent: 0.1% aqueous formic acid [A] and acetonitrile with 0.1% formic acid [B] using a linear gradient of 5% B to 95% B over 17 min in combination with an LCQ Fleet mass spectrometer). Solutions of DK325 and DK359 (40 µM) in kinase assay buffer or cell medium were irradiated with UV lamp (Spectroline, ENB-280C/FE, 1x8 Watt) or violet light (3 x 1000 mW, λ_{max} = 400 nm, FWHM 11.9 nm, Sahlmann Photochemical Solutions) from 10 cm distance, and aliquots (final concentration of 20 µM) were taken for UPLC-MS analysis.

Chemical actinometry

A modification of a standard protocol was applied for the determination of the photon flux.[15] An aqueous H_2SO_4 solution (0.05 M) containing $K_3[Fe(C_2O_4)_3]$ (41 mM, 2 mL, 1 cm quartz cuvette) was irradiated at 20 °C for a given period of time in the dark with a 365 nm LED. The solution was then diluted with 1.0 mL of an aqueous H_2SO_4 solution (0.5 M) containing phenanthroline (1 g/L) and NaOAc (122.5 g/L). The absorption at λ= 510 nm was measured and compared to an identically prepared non-irradiated sample. The concentration of $[Fe(phenanthroline)_3]^{2+}$ complex was calculated using its molar absorptivity (ε = 11100 M^{-1} cm^{-1}) and taking into account the dilution. The quantity of Fe^{2+} ions expressed in mol was plotted versus time (expressed in seconds) and the slope, obtained by linear fitting the data points to the equation y = ax +b using Origin software, equals the rate of formation of the Fe^{2+} ion at the given wavelength in standardized conditions. This rate can be converted into the photon flux (I) by dividing it by the quantum yield of $[Fe(phenanthroline)_3]^{2+}$ complex (Φ_{365nm} = 1.29) at 365 nm and by the probability of photon absorption at 365 nm of the Fe^{3+} complex (approximated to 1, because the absorbance of $K_3[Fe(C_2O_4)_3]$ at 365 nm is greater than 2). The obtained photon flux is: I = 4.059x10^{-5} einstein s^{-1}.

Quantum yield measurement

The quantum yields of the compounds were determined following the photo-deprotection process by UPLC-MS (ThermoFischer Scientific Vanquish UPLC System; C18 column: Acquity UPLC HSS T3 1.8 µm, 2.1 × 150 mm; eluent: 0.1% aqueous formic acid [A] and acetonitrile with 0.1% formic acid [B] using a linear gradient of 5% B to 95% B over 17 min in combination with an LCQ Fleet mass spectrometer). Solutions of DK325 (10 mM) and DK359 (400 µM) in DMSO (3 ml) in quartz cuvettes were vigorously stirred with a stirring egg in order to keep a homogenous solution. Temperature was kept constant at 25 °C. Mentioned concentrations enabled us to work in high-absorption regime (absorbance at 365 nm ≥ 2), and make an assumption that all incident photons are absorbed. Irradiation with a multi-wavelength fiber coupled LED-system (FC6-LED-WL) using 365A LED was conducted in precisely measured time intervals. Aliquots of 4 µl (DK325) or 20 µl (DK359) of the irradiated solutions were transferred to a vial with a 996 µL or 180 µL acetonitrile in order to obtain 40 µM solution. The amount of the photo-deprotected substrate was quantified measuring the peak area in UPLC traces and using the calibration curve. The resulting quantum yields were determined using the following equation and data from Figure S4:

$$\frac{\Delta c \times V}{\Delta t \times I} = \Phi$$

In vitro kinase assay

The *in vitro* kinase activity assay was conducted as described previously[16] with modifications for the irradiation experiments. The assays were performed on a white, solid-bottom 384-well plates (10 µl volume). The reaction mixture was as follows: 1 ng/µl CKIα (Invitrogen, PV3850), 50 µM RRKDLHDDEEDEAMSITA peptide substrate (Anaspec, 60547-1), and CKI buffer (40 mM Tris-HCl, 10 mM $MgCl_2$, 0.5 mM DTT, and 0.1 mg/ml BSA). For the reaction with CKIδ was used: 0.6 ng/µl CKIδ (Merck Millipore 14-520), 50 µM RKKKAEpSVASLTSQCSYSS peptide substrate (Anaspec, custom made), and CKI buffer. Solution containing the small molecule in DMSO was pipetted into the wells (0.5 µl, final 5% DMSO). Afterwards, 1 µl of a 50 µM ATP solution was pipetted into the upper corner of each well, and the enzymatic reaction was started by spinning down the plate (3000 rpm, 2 min). By employing this method, all reactions were started at the same time, minimizing variance between different samples. A calibration curve was set up employing 9 µL of the CKI buffer, 0.5 µL DMSO and 1 µl of a dilution series of ATP (50, 40, 30, 20 and 10 µM, respectively). Incubation for 3 h at 30 °C allowed for the enzymatic phosphorylation of the substrate peptide. As the reaction started, the wells were irradiated with UV lamp (Spectroline, ENB-280C/FE, 1x8 Watt) or violet lamp (3 x 1000 mW, λ_{max} = 400 nm, FWHM 11.9 nm, Sahlmann Photochemical Solutions) for different duration followed by sealing off the wells with an aluminum sticker to shield from irradiation. Dark (0 min irradiation) wells were covered with an aluminium sticker from the beginning. After the incubation period (3 h), 10 µL Kinase Glo (Promega) was pipetted into the wells. To stabilize the luminescent signal, the plate was incubated for 10 min at room temperature, after which the luminescent signal was recorded by a plate reader (BioTek Synergy H1). A calibration curve was set up correlating luminescence intensity with ATP concentration. The ATP consumption in DMSO control samples, containing the enzyme and peptide substrate without inhibitor, was set at 100% enzyme activity.

Cellular circadian assay

Effects of compounds on cellular circadian rhythms were analyzed as described previously[1] with modifications. Stable U2OS reporter cells harboring *Bmal1-dLuc* reporter were suspended in phenol red-free culture medium [DMEM (D2902, Sigma) supplemented with 10% fetal bovine serum, 3.5 mg/ml D-glucose, 3.7 mg/ml sodium bicarbonate, 0.29 mg/ml L-glutamine, 100 units/ml penicillin, and 100 µg/ml streptomycin] and plated onto a white, solid-bottom 384-well plates at 30 µl (3,000 cells) per well. After 2 days, 40 µl of phenol red-free explant medium [DMEM (D2902, Sigma) supplemented with 2% B27 (Gibco), 10 mM HEPES, 3.5 mg/ml D-glucose, 0.38 mg/ml sodium bicarbonate, 0.29 mg/ml L-glutamine, 100 units/ml penicillin, 100 µg/ml streptomycin, and 0.2 mM luciferin; pH 7.2] was dispensed into each well, followed by the application of 500 nl of compounds (dissolved in DMSO; final 0.7% DMSO). The plate was covered with an optically clear film, and subjected to irradiation with 365 nm UV lamp (SLUV-6, AS ONE) from 10 cm distance or 400 nm LED lamp (3 x 1000 mW, λ_{max} = 400 nm, FWHM 11.9 nm, Sahlmann Photochemical Solutions) from 12 cm distance. Luminescence was recorded every 100 min in a microplate reader, Infinite M200Pro (Tecan).

Ex vivo circadian studies

Spleen tissue was dissected from *Per2::Luc* knockin mice[2] and analyzed as described previously[17] with modifications. Tissue pieces were cultured in phenol red-free explant medium without luciferin and containing compounds (final 0.24% DMSO) in a black, clear-bottom 24-well plate. The plate was covered with an optically clear film, and subjected to irradiation with 400 nm LED lamp from 12 cm distance. Luciferin (final 1 mM) was supplemented to the medium, and luminescence was recorded every 30 min for 5 days in a LumiCEC luminometer (Churitsu). Circadian period was determined from luminescence rhythms by a curve fitting program MultiCycle (Actimetrics). Data from the first day was excluded from analysis, because of transient changes in luminescence upon medium change.

To harvest the suprachiasmatic nucleus (SCN), *Per2::Luc* heterozygote neonatal mice at postnatal day four or five were euthanized. Coronal SCN slices of 300 µm thick were made with a tissue chopper (Mcllwain). The SCN tissue was dissected at the mid-rostrocaudal region and a paired SCN was cultured on a Millicell-CM culture insert (Millipore Corporation). The culture conditions were the same as those described previously.[18] Briefly, the slice was cultured in air at 36.5 ºC with 1 ml DMEM (Invitrogen) containing 0.1 mM D-luciferin

(Wako Pure Chemical) and 5 % fetal bovine serum for three or four days, and then measurement of *Per2::Luc* bioluminescence was started by using luminometor (Kronos, Atto). DK359 (final 24 μM) or vehicle (DMSO) was applied into the culture medium from the beginning of the measurement. Four to five days after starting measurement, the tissue was subjected to irradiation with 400 nm LED lamp from 11 cm distance. Circadian period was calculated by a Chi-square periodogram (ClockLab). The analysis was applied for a record data of four or five consecutive days with a significance level of $P = 0.01$.

Zebrafish experiment

Larval fish were entrained under 12 h light/12 h dark cycles for 4 d under a constant temperature of 28 °C (Percival light incubator I-41LL). On day 4, they were placed in an individual well of a 96-well white solid-bottom plate with 325 μL of E3 solution (aq. 5 mM NaCl, 0.17 mM KCl, 0.33 mM $CaCl_2$, and 0.33 mM $MgSO_4$, pH 7.0). The plate was covered with optically clear film. On day 5, the lighting condition was changed to constant darkness until the end of the experiment on day 7 (6 dpf). At CT6 on day 5, the compounds diluted in E3 and pre-arrayed in a 96 well plate were transferred to the larva plate using a BenchTop 96-well Pipettor (Sorenson Bioscience) in darkness. Light treatment for compound activation using 400 nm LED (3 x 1000 mW, λ_{max} = 400 nm, FWHM 11.9 nm, Sahlmann Photochemical Solutions) was performed inside the incubator for 5 and 10 min using 10 cm distance. A section of the plate was covered with aluminum foil for the dark treatment. Following illumination, luciferin (final 0.2 mM) was added from a pre-arrayed plate using the 96-well pipettor. The plate was then sealed and placed in the Molecular Device LMAX II384 for bioluminescence reading. The plate was read every 30 minutes. After completing a read, the reader plate holder was maintained opened for temperature uniformity with the chamber using a python script controlling the Softmax Pro software. The data files were converted using a python script for processing with BioDare2 (biodare2.ed.ac.uk) for period estimation and visualization.[19] The data from CT10 to CT75 was selected and processed using detrending for baseline and amplitude.

QUANTIFICATION AND STATISTICAL ANALYSIS

Statistical significance was evaluated using one-way or two-way ANOVA, followed by a Tukey's multiple comparisons test using Prism software (GraphPad Software).

SUPPLEMENTAL FIGURES

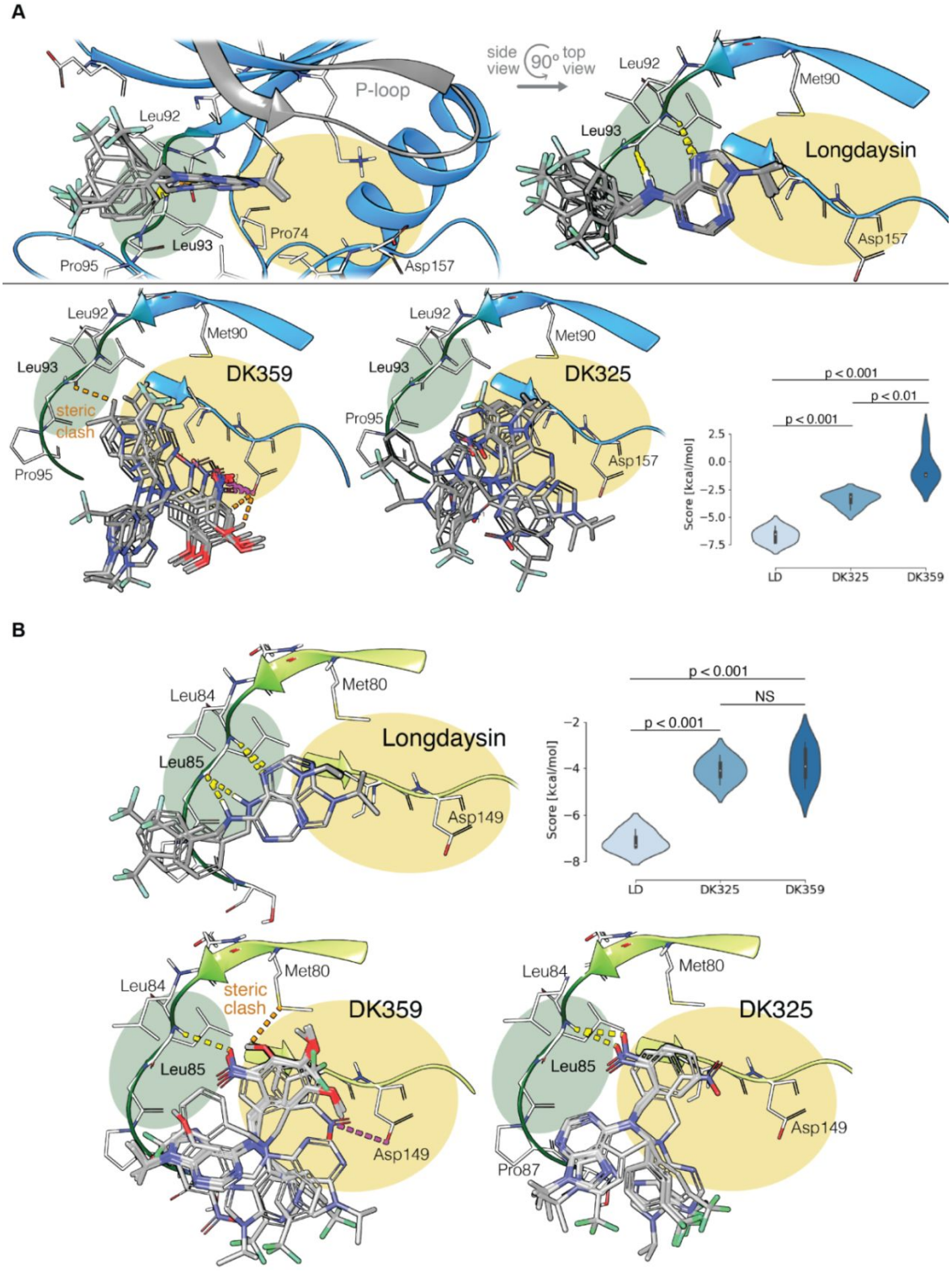

Figure S1. Docking Conformations of Longdaysin, DK325, and DK359 to CKIα and CKIδ. **(A)** The top 5 scored docking conformations of longdaysin (upper panel) and DK325 and DK359 (lower panel) to CKIα. Hydrogen bonds, steric clashes, and ionic interactions are indicated as yellow, orange, and magenta dashed lines,

respectively. The CKIα binding site is characterized by a kinase-specific hinge region (green) and an adjacent cavity formed by the p-loop (yellow). Hypothesis testing was performed using ANOVA and Tukey's test post-hoc analysis (bottom right panel). LD = longdaysin. **(B)** All 3 docked conformations of longdaysin (upper panel) and top 5 scored docking conformations of DK325 and DK359 (lower panel) to CKIδ. Hydrogen bonds, steric clashes, and ionic interactions are indicated as yellow, orange, and magenta dashed lines, respectively. The CKIδ binding site is characterized by a kinase-specific hinge region (green) and an adjacent cavity formed by the p-loop (yellow). Hypothesis testing was performed using ANOVA and Tukey's test post hoc analysis (top right panel). LD = longdaysin; NS = not significant.

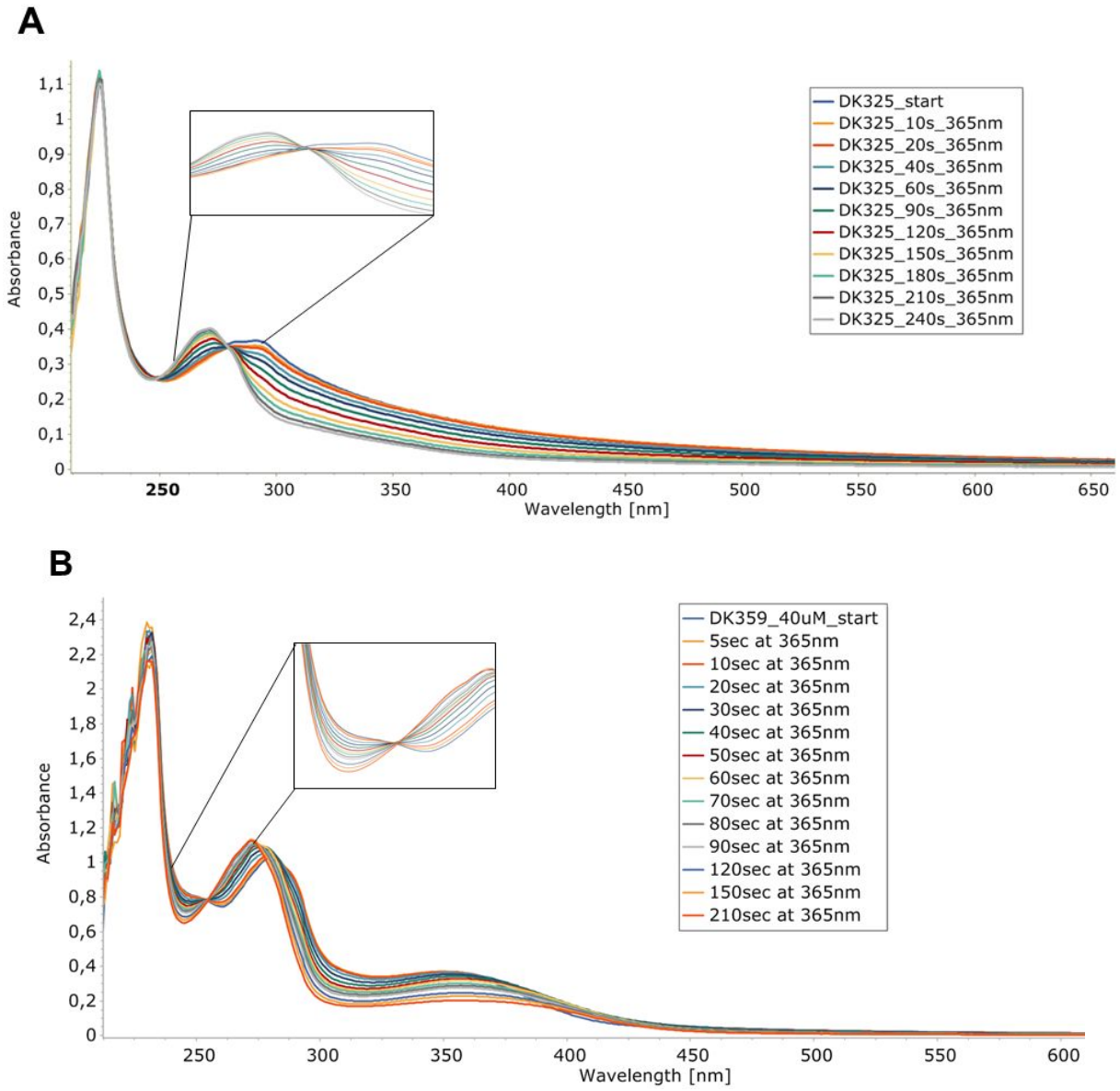

Figure S2. UV-Vis spectroscopy analysis of photo-deprotection of DK325 and DK359 (40 μM in buffer, 30 °C) showing clear isosbestic points.

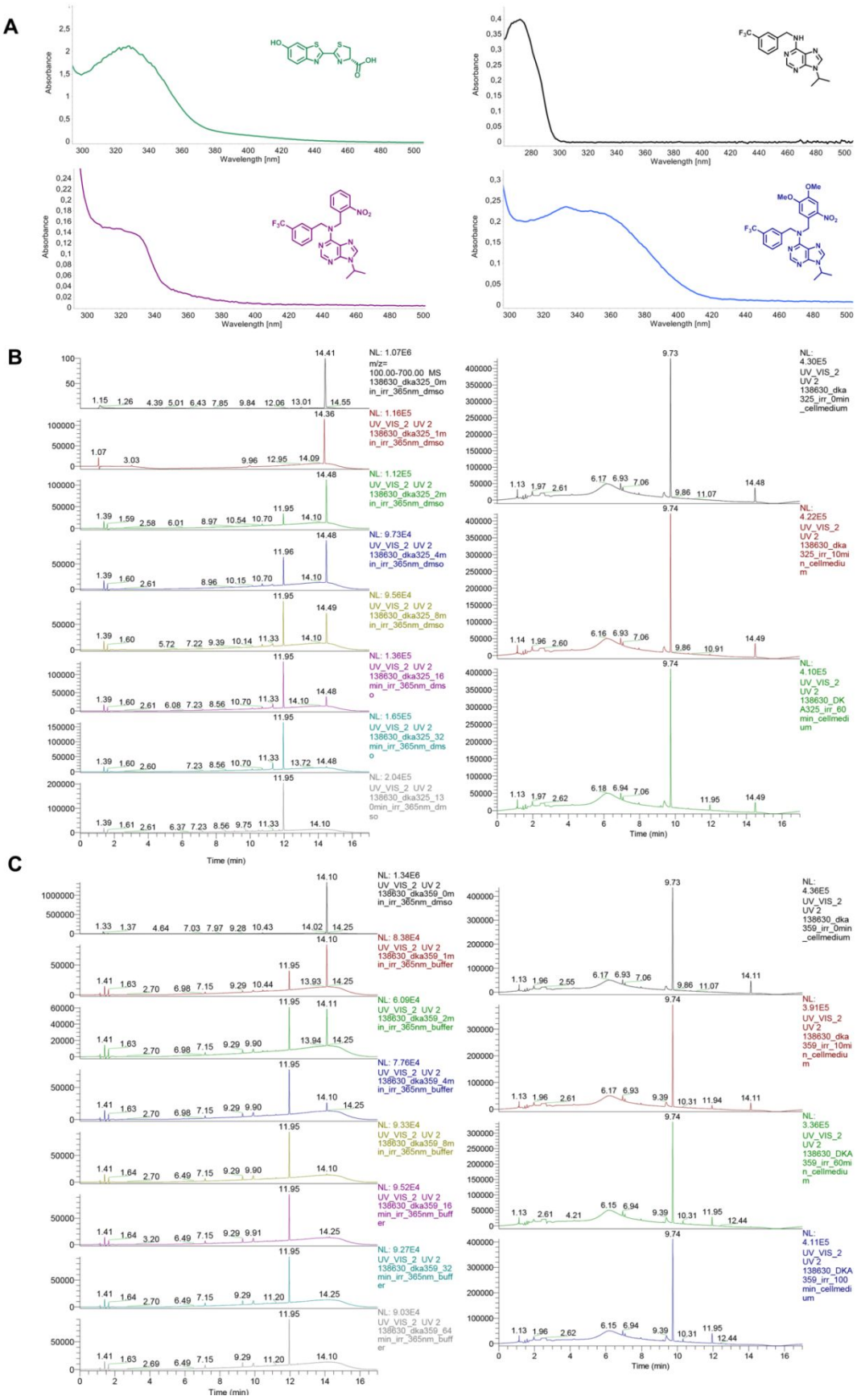
A
B
C
Absorbance
Wavelength [nm]
Time (min)

Figure S3. In vitro Photo-deprotection Studies of DK325 and DK359. **(A)** UV spectrum of luciferin (0.1 mM in kinase buffer, λ_{max} = 330 nm), longdaysin (40 μM in DMSO, λ_{max} = 273 nm), DK325 (40 μM in DMSO, λ_{max} = 320 nm), and DK359 (40 μM in DMSO, λ_{max} = 345 nm). **(B)** UPLC chromatograms of DK325 upon irradiation in kinase assay buffer (40 μM; UV-light, λ_{max} = 365 nm; 0 min, 1 min, 2 min, 4 min, 8 min, 16 min, 32 min and 130 min) and cellular medium (40 μM; visible light, λ_{max} = 400 nm; 0 min, 10 min, and 60 min). Retention time (min) is shown on the x-axis. Shown are the peaks of luciferin (9.73-9.74 min), longdaysin (11.95 min) and DK325 (14.36-14.49 min). **(C)** UPLC chromatograms of DK359 upon irradiation in kinase assay buffer (40 μM; UV-light, λ_{max} = 365 nm; 0 min, 1 min, 2 min, 4 min, 8 min, 16 min, 32 min and 64 min) and cellular medium (40 μM; visible light, λ_{max} = 400 nm; 0 min, 10 min, 60 min, and 100 min). Retention time (min) is shown on the x-axis. Shown are the peaks of luciferin (9.73-9.74 min), longdaysin (11.94-11.95 min), and DK359 (14.11 min).

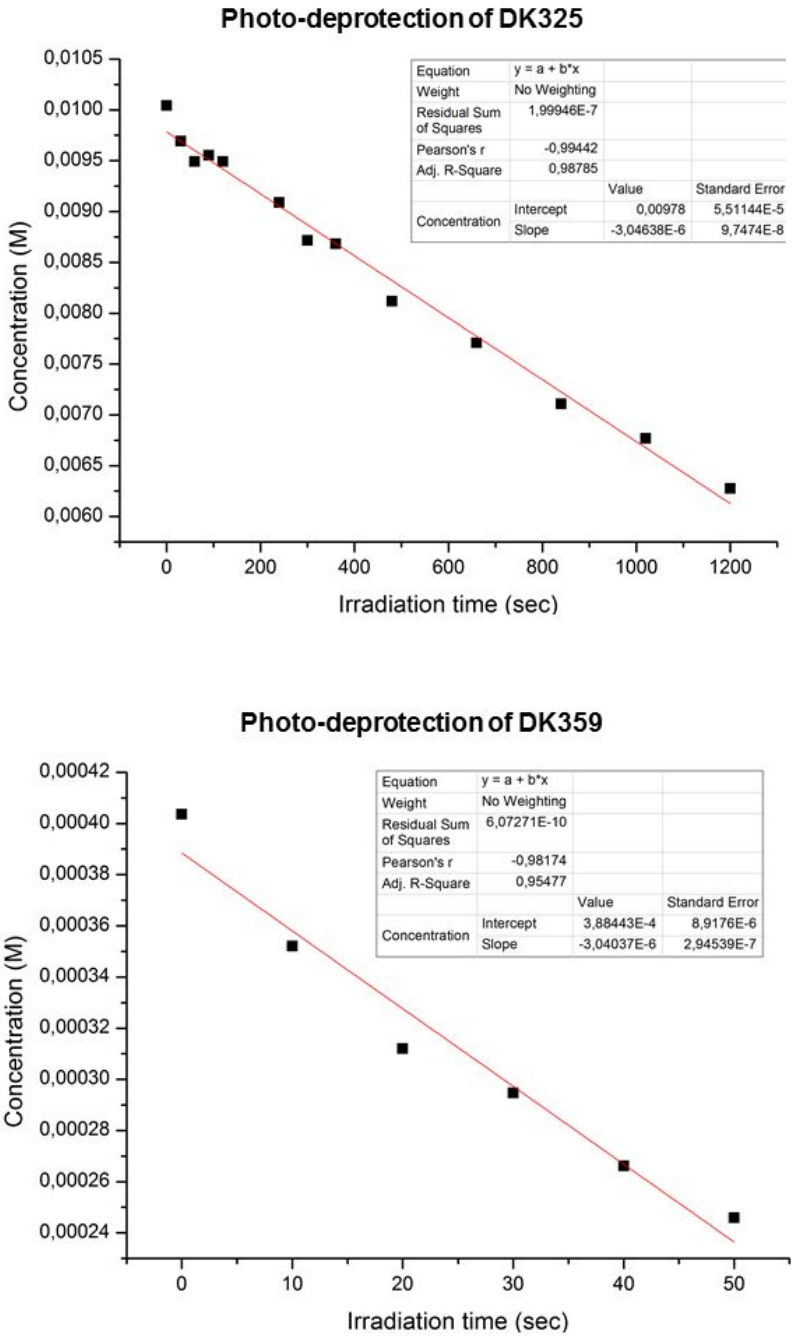

Figure S4. Plot of the concentration of DK325 and DK359 as a function of time during λ_{max} = 365 nm irradiation obtained by monitoring the peak area in UPLC traces (at λ = 254 nm). The slope of the plot corresponds to the rate of DK325 and DK359 photo-deprotection rate: 3.05×10^{-6} M $s^{-1} \pm 9.75 \times 10^{-8}$ M s^{-1} and 3.04×10^{-6} M $s^{-1} \pm 2.95 \times 10^{-7}$ M s^{-1}. Correlation of this rate to the photon flux ($I = 4.06 \times 10^{-5}$ mol s^{-1} ml^{-1}) gives quantum yields of 22.51% for DK325 and 22.47% for DK359.

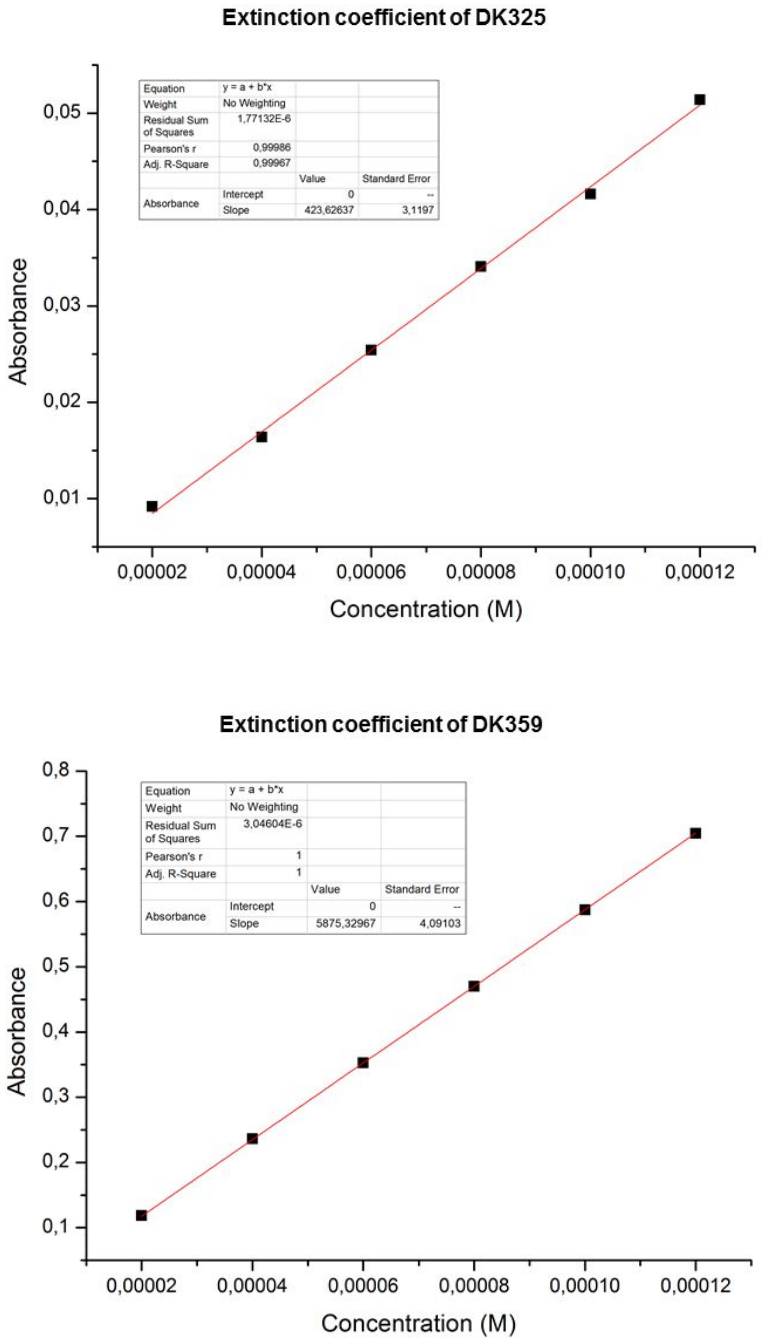

Figure S5. Determination of the molar extinction coefficient for DK325 and DK359. ε_{365}(DK325) = 424 M^{-1} cm^{-1} and ε_{365}(DK359) = 5875 M^{-1} cm^{-1}.

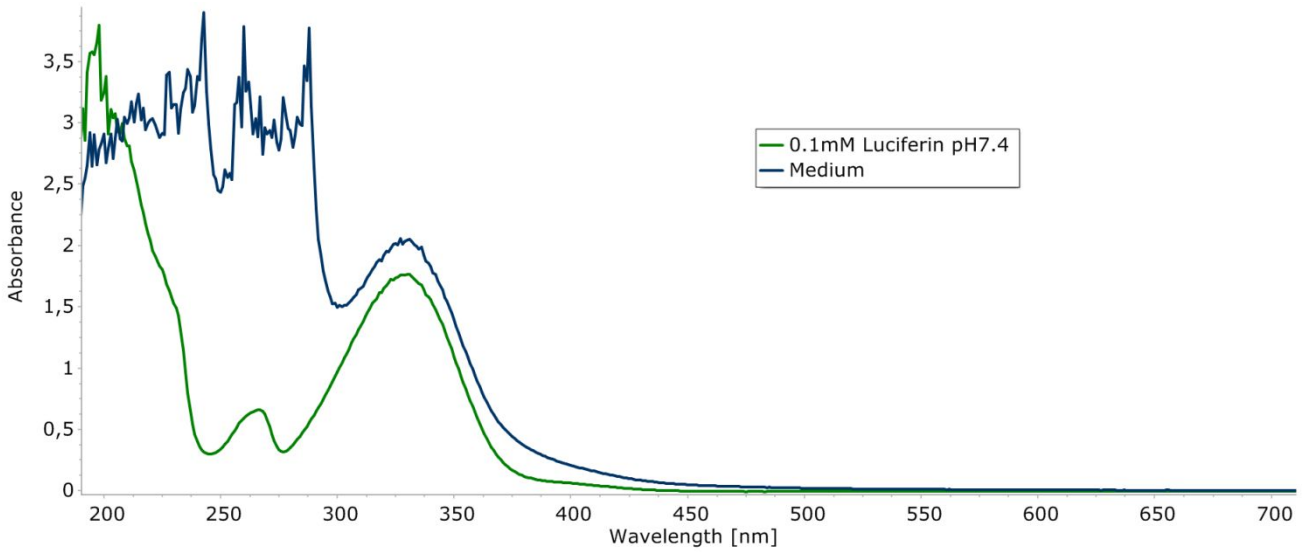

Figure S6. Absorption spectrum of luciferin at pH 7.4 (0.1 mM in water) and of cellular medium containing luciferin (0.1 mM).

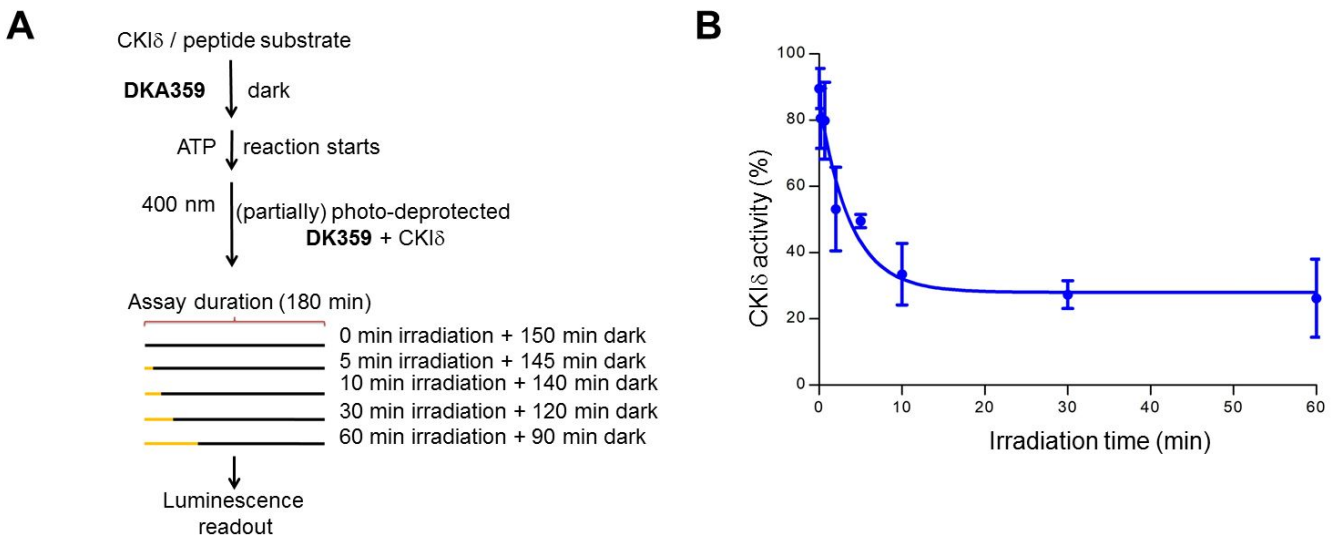

Figure S7. Inhibition of CK1δ in a Light-Dependent Manner. **(A)** DK359 (40 μM final concentration) was applied to CKIδ-reaction mixture. The release of longdaysin was controlled by different irradiation duration (0 – 60 min) after the reaction was initiated by the addition of ATP and peptide substrate. **(B)** *In situ* irradiation results. Degree of CK1δ inhibition was plotted against irradiation time of violet light, λ = 400 nm. The ATP consumption in DMSO control samples, containing the enzyme and peptide substrate without inhibitor, was set at 100% enzyme activity.

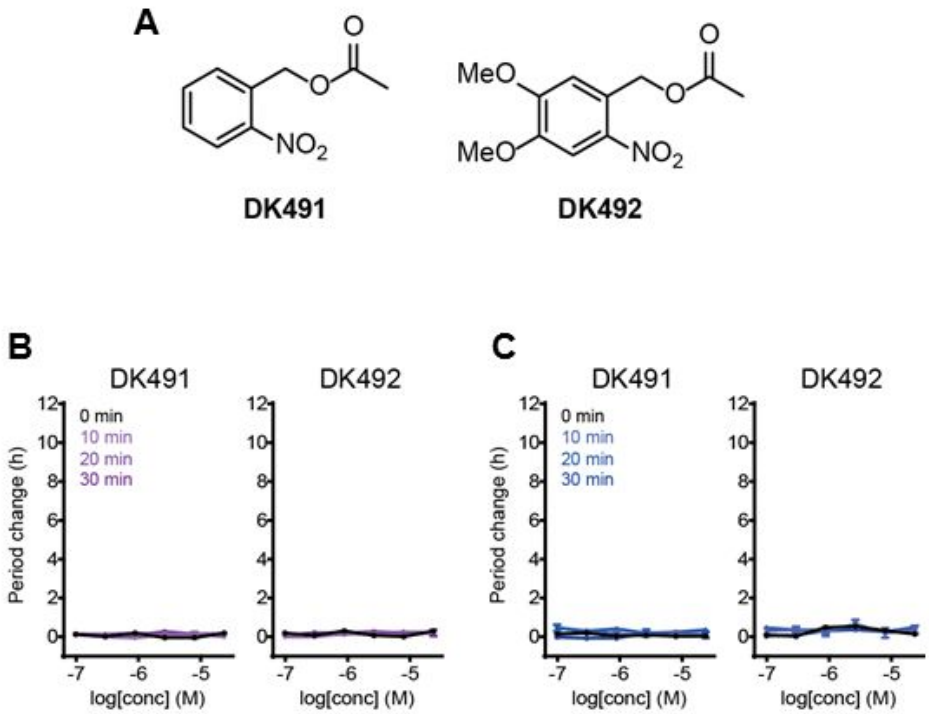

Figure S8. Period Change of DK491- and DK492-Treated Cells. **(A)** Chemical structures of the control compounds DK491 and DK492. **(B and C)** Effect of photo-deprotection side products on cellular period change. *Bmal1-dLuc* reporter cells were treated with various concentrations of compound (6 points of 3-fold dilution series in DMSO) and irradiated with 365 nm light **(B)** or 400 nm light **(C)** for 0 to 30 min. Luminescence rhythms were then monitored and period change was calculated (n = 4).

Figure 4A

DK325

	log[conc] (M)					
	-7.01	-6.53	-6.05	-5.58	-5.10	-4.62
1 min	ns	ns	ns	ns	ns	*
2 min	ns	ns	ns	ns	ns	**
10 min	ns	ns	ns	ns	ns	****
20 min	ns	ns	ns	ns	**	****
30 min	ns	ns	ns	ns	****	****

DK359

	log[conc] (M)					
	-7.01	-6.53	-6.05	-5.58	-5.10	-4.62
1 min	ns	ns	ns	ns	ns	**
2 min	ns	ns	ns	ns	ns	****
10 min	ns	ns	ns	ns	****	****
20 min	ns	ns	*	****	****	****
30 min	ns	ns	**	****	****	****

Longdaysin

	log[conc] (M)			
	-7.01	-6.53	-6.05	-5.58
10 min	ns	ns	ns	ns
20 min	ns	ns	ns	ns
30 min	ns	ns	ns	ns

Figure 4B

DK325

	log[conc] (M)					
	-7.01	-6.53	-6.05	-5.58	-5.10	-4.62
1 min	ns	ns	ns	ns	ns	*
2 min	ns	ns	ns	ns	ns	****
10 min	ns	ns	ns	ns	**	****
20 min	ns	ns	**	****	****	****
30 min	ns	*	**	****	****	****

DK359

	log[conc] (M)					
	-7.01	-6.53	-6.05	-5.58	-5.10	-4.62
1 min	ns	ns	ns	ns	ns	****
2 min	ns	ns	ns	ns	***	****
10 min	ns	ns	**	***	****	****
20 min	ns	*	****	****	****	
30 min	ns	**	****	****	****	

Longdaysin

	log[conc] (M)			
	-7.01	-6.53	-6.05	-5.58
10 min	ns	ns	ns	ns
20 min	ns	ns	ns	ns
30 min	ns	ns	ns	ns

Figure 4C

DK325-pre

	log[conc] (M)					
	-7.01	-6.53	-6.05	-5.58	-5.10	-4.62
5 min	ns	ns	ns	ns	ns	*
15 min	ns	ns	ns	ns	ns	ns
30 min	ns	ns	ns	ns	ns	ns

DK359-pre

	log[conc] (M)					
	-7.01	-6.53	-6.05	-5.58	-5.10	-4.62
5 min	ns	ns	ns	ns	ns	ns
15 min	ns	ns	ns	ns	ns	ns
30 min	ns	ns	ns	ns	ns	ns

Longdaysin-pre

	log[conc] (M)			
	-7.01	-6.53	-6.05	-5.58
5 min	ns	ns	ns	ns
15 min	ns	ns	ns	ns
30 min	ns	ns	ns	ns

DK325-post

	log[conc] (M)					
	-7.01	-6.53	-6.05	-5.58	-5.10	-4.62
5 min	ns	ns	ns	ns	ns	****
15 min	ns	ns	ns	****	****	****
30 min	ns	ns	ns	****	****	

DK359-post

	log[conc] (M)					
	-7.01	-6.53	-6.05	-5.58	-5.10	-4.62
5 min	ns	ns	ns	****	****	****
15 min	ns	ns	****	****	****	
30 min	ns	*	****	****		

Longdaysin-post

	log[conc] (M)			
	-7.01	-6.53	-6.05	-5.58
5 min	ns	ns	ns	ns
15 min	ns	ns	*	ns
30 min	ns	ns	**	ns

Table S1. Statistical Analysis. ****$p < 0.0001$, ***$p < 0.001$, **$p < 0.01$, *$p < 0.05$ against the DMSO control.

NMR DATA

N-(2-nitrobenzyl)-1-(3-(trifluoromethyl)phenyl)methanamine

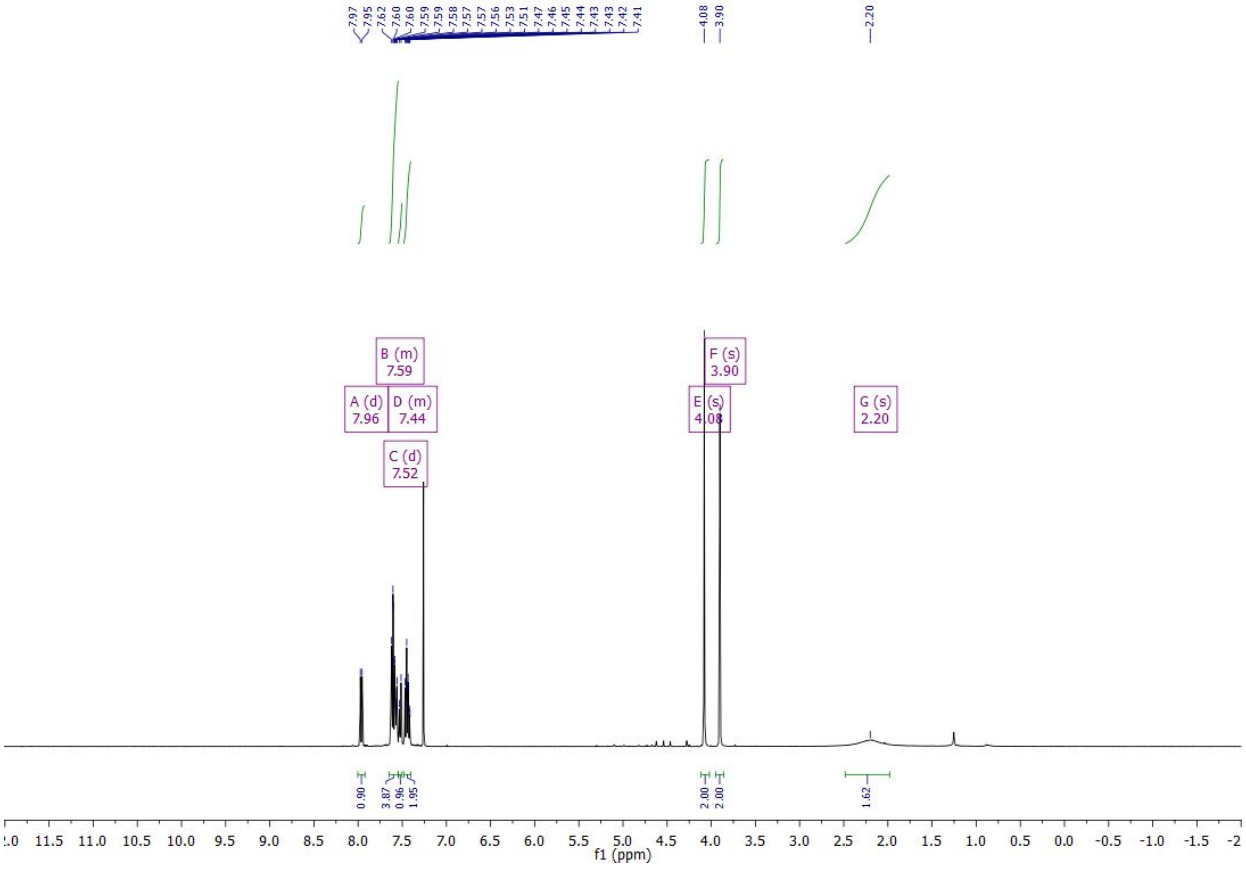

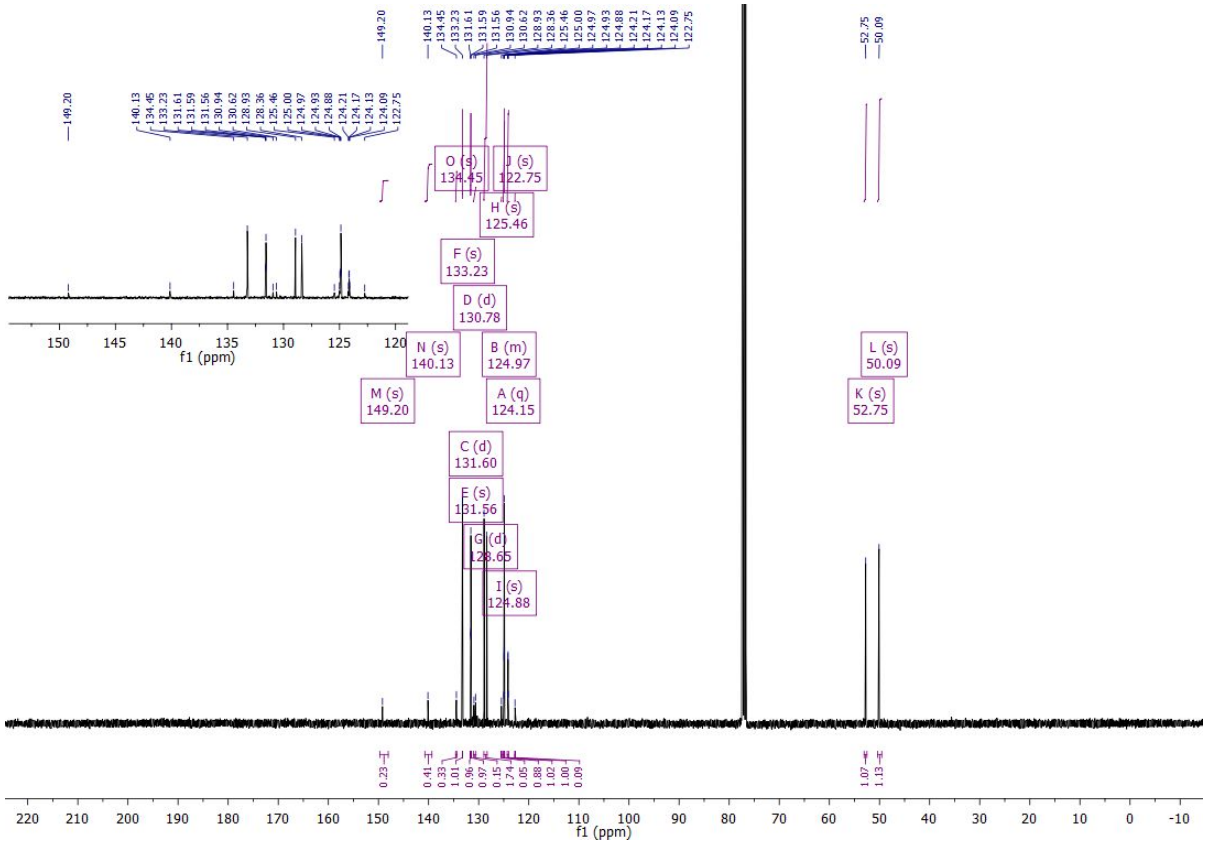
O (s) 134.45
J (s) 122.75
H (s) 125.46
F (s) 133.23
D (d) 130.78
N (s) 140.13
B (m) 124.97
M (s) 149.20
A (q) 124.15
C (d) 131.60
E (s) 131.56
G (d) 128.65
I (s) 124.88
L (s) 50.09
K (s) 52.75
f1 (ppm)

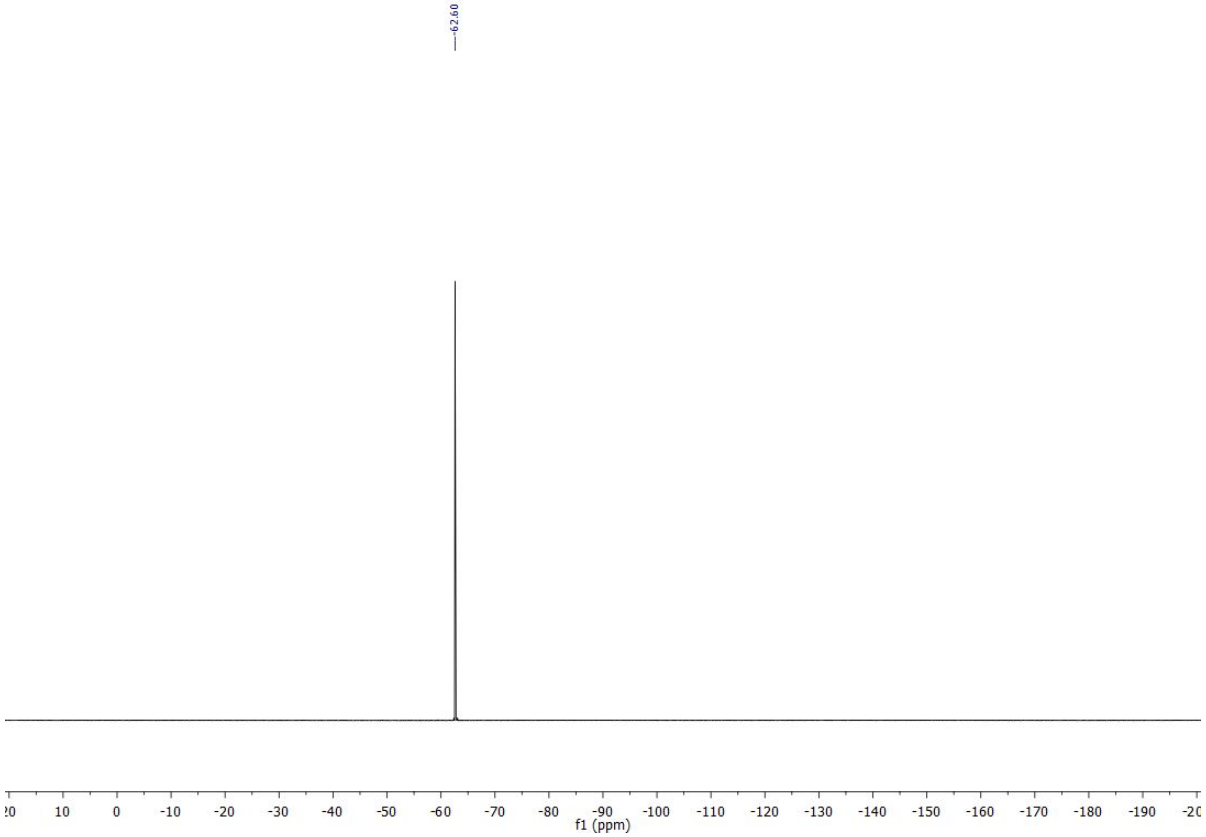
-62.60
f1 (ppm)

N-(4,5-dimethoxy-2-nitrobenzyl)-1-(3-(trifluoromethyl)phenyl)methanamine

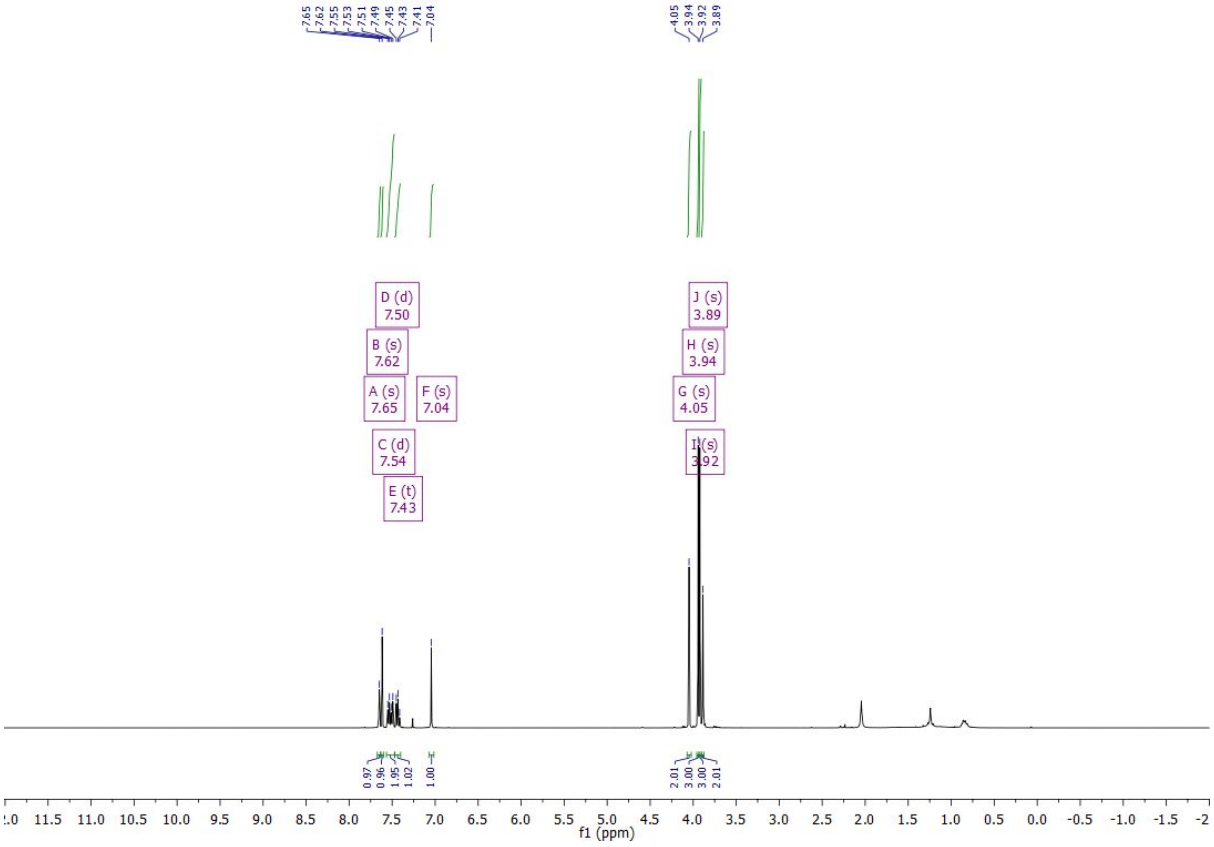

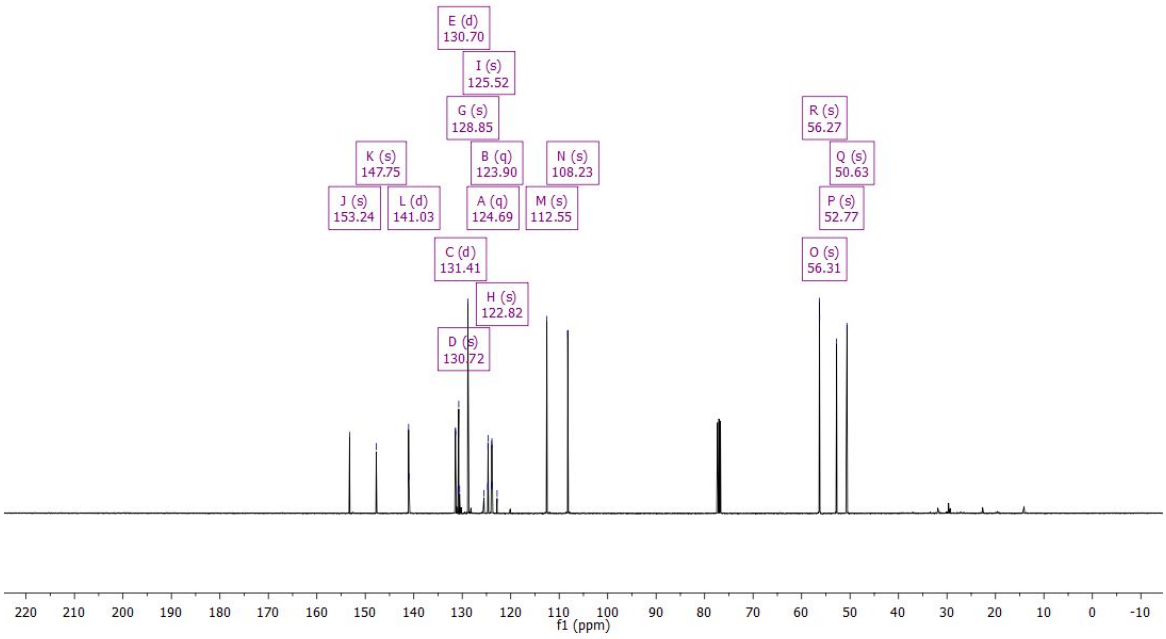

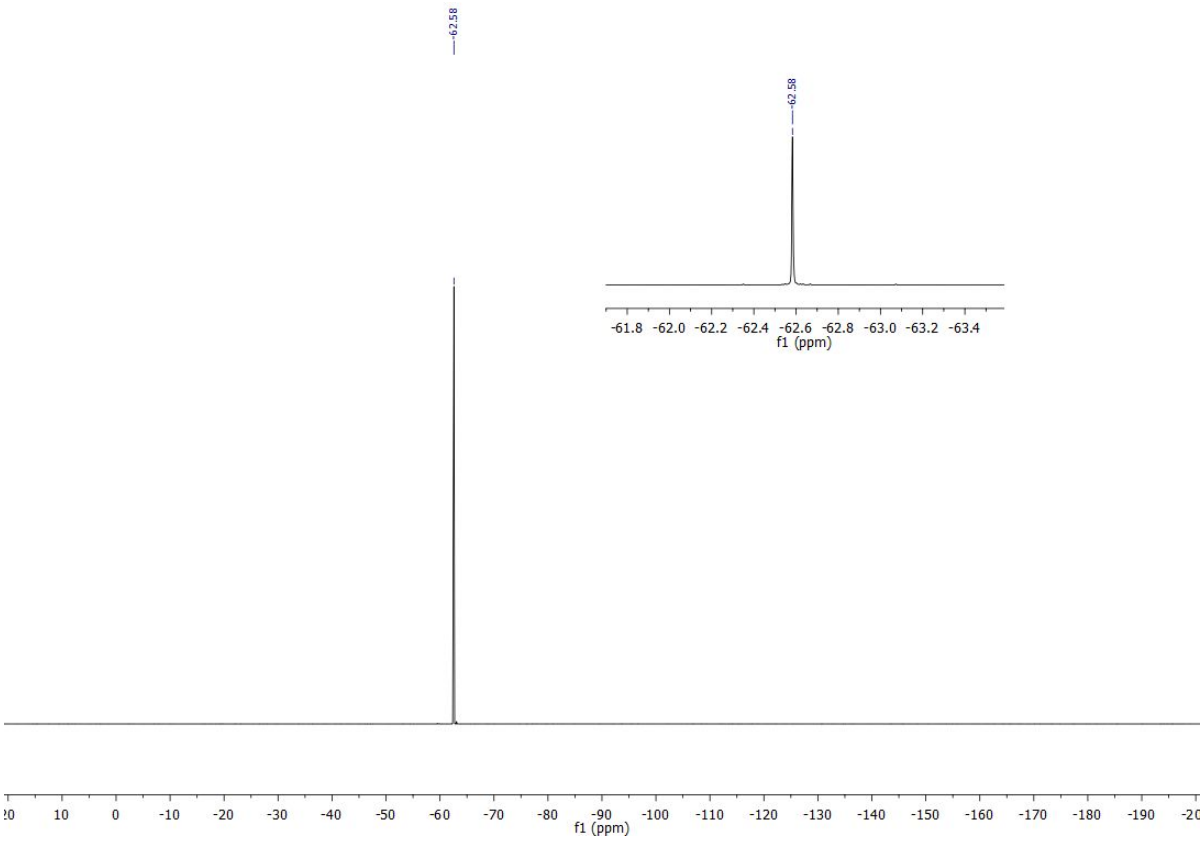
-62.58
-62.58
-61.8 -62.0 -62.2 -62.4 -62.6 -62.8 -63.0 -63.2 -63.4
f1 (ppm)
10 0 -10 -20 -30 -40 -50 -60 -70 -80 -90 -100 -110 -120 -130 -140 -150 -160 -170 -180 -190
f1 (ppm)

9-isopropyl-N-(2-nitrobenzyl)-N-(3-(trifluoromethyl)benzyl)-9H-purin-6-amine (DK325)

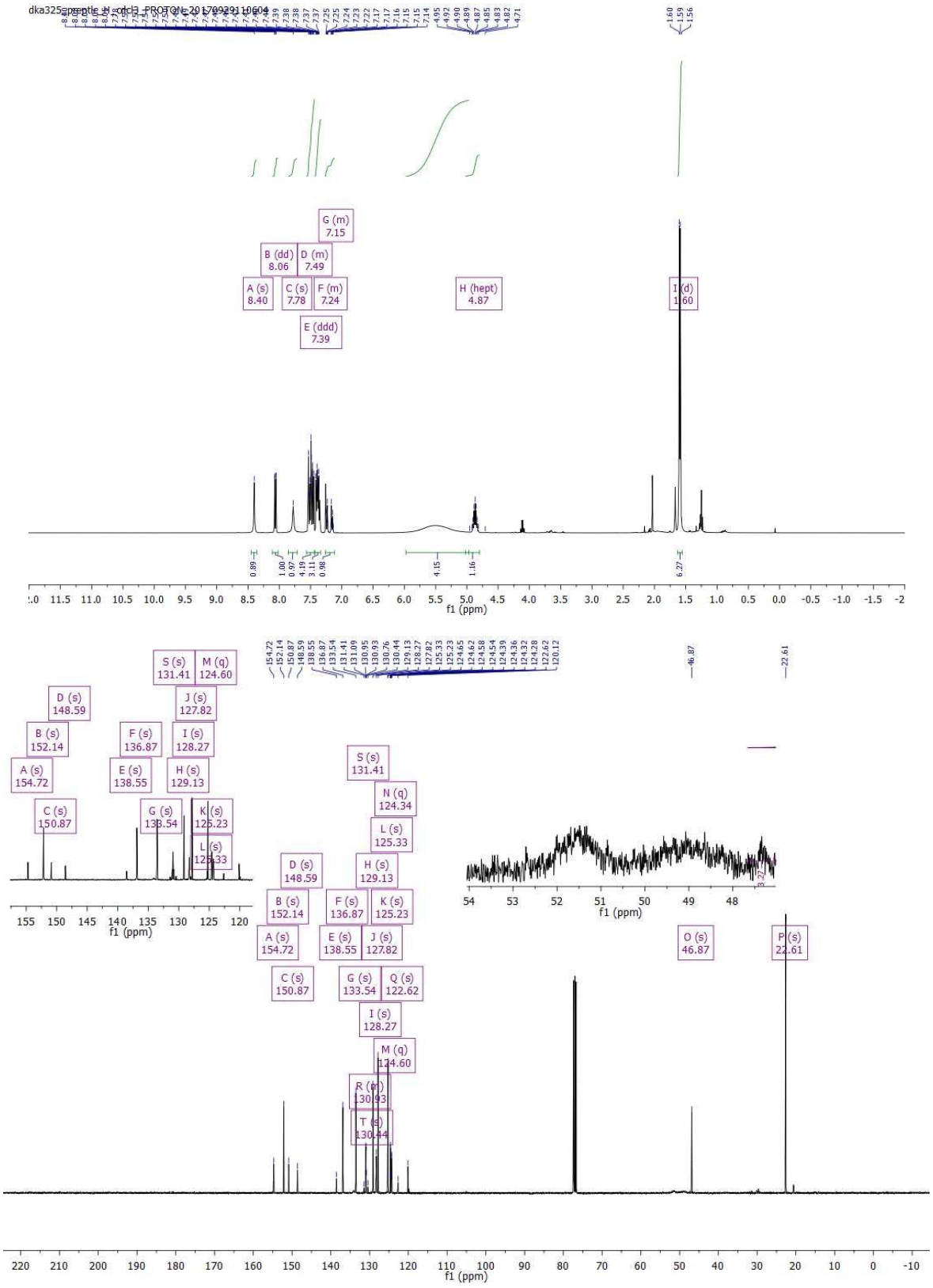

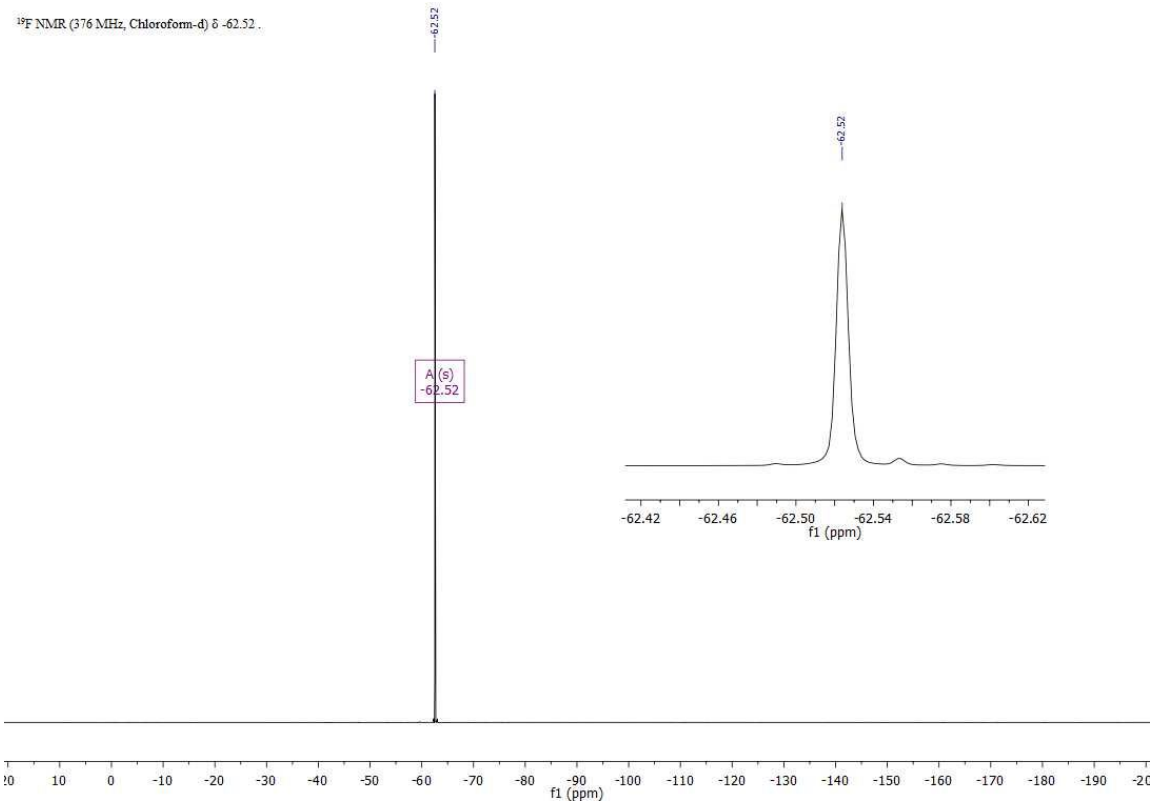
^{19}F NMR (376 MHz, Chloroform-d) δ -62.52 .
-62.52
A (s)
-62.52
-62.52
-62.42
-62.46
-62.50
-62.54
-62.58
-62.62
f1 (ppm)
10
0
-10
-20
-30
-40
-50
-60
-70
-80
-90
-100
-110
-120
-130
-140
-150
-160
-170
-180
-190
f1 (ppm)

N-(4,5-dimethoxy-2-nitrobenzyl)-9-isopropyl-N-(3-(trifluoromethyl)benzyl)-9H-purin-6-amine (DK359)

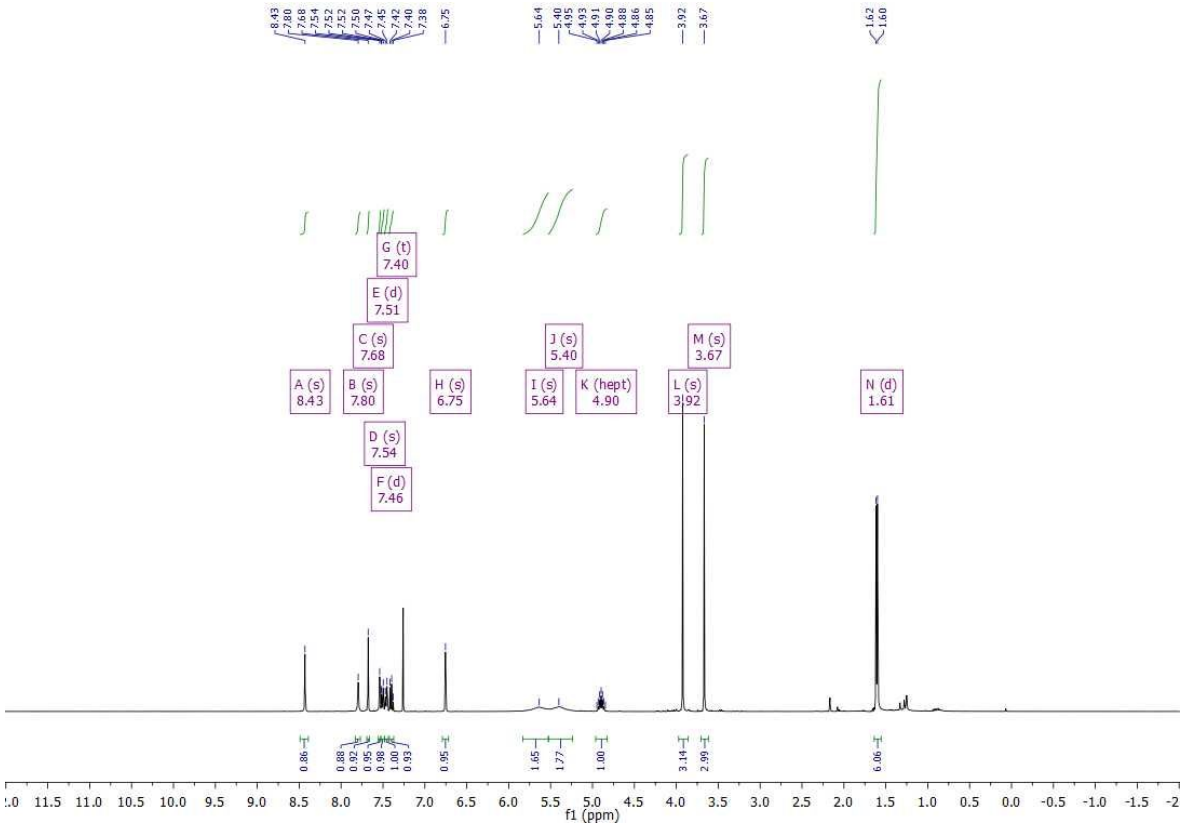

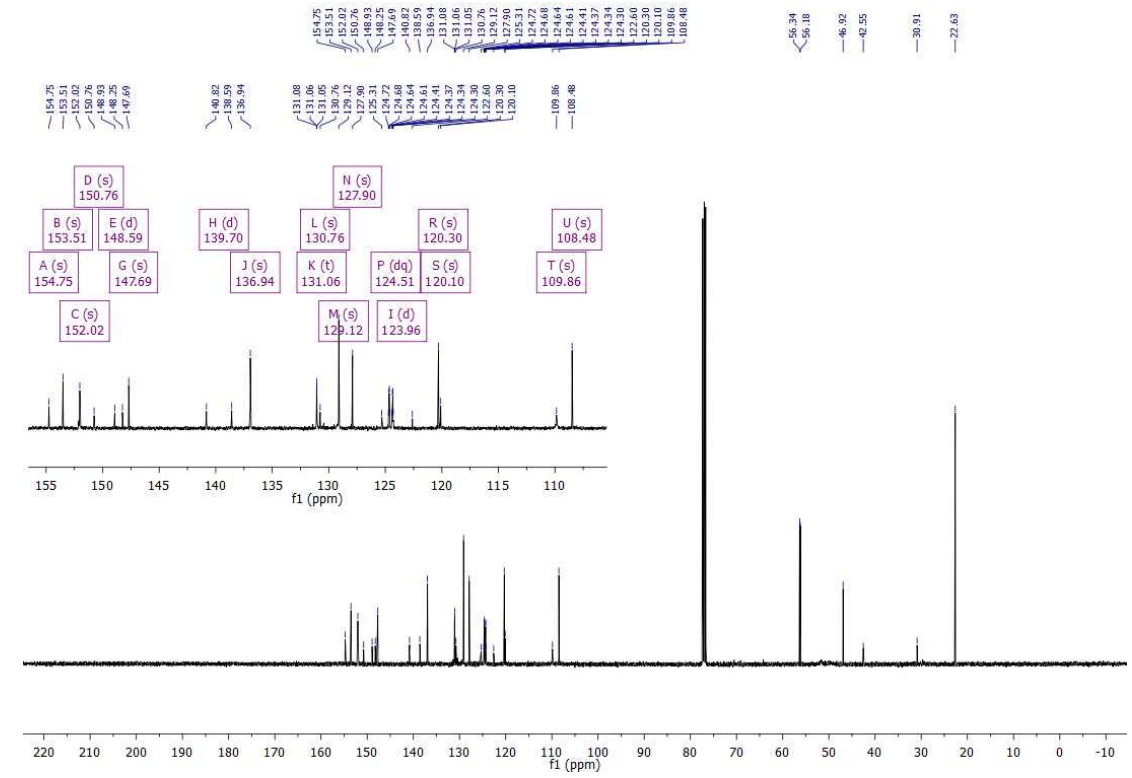
D (s) 150.76
B (s) 153.51
E (d) 148.59
H (d) 139.70
L (s) 130.76
N (s) 127.90
R (s) 120.30
U (s) 108.48
A (s) 154.75
G (s) 147.69
J (s) 136.94
K (t) 131.06
P (dq) 124.51
S (s) 120.10
T (s) 109.86
C (s) 152.02
M (s) 129.12
I (d) 123.96
f1 (ppm)

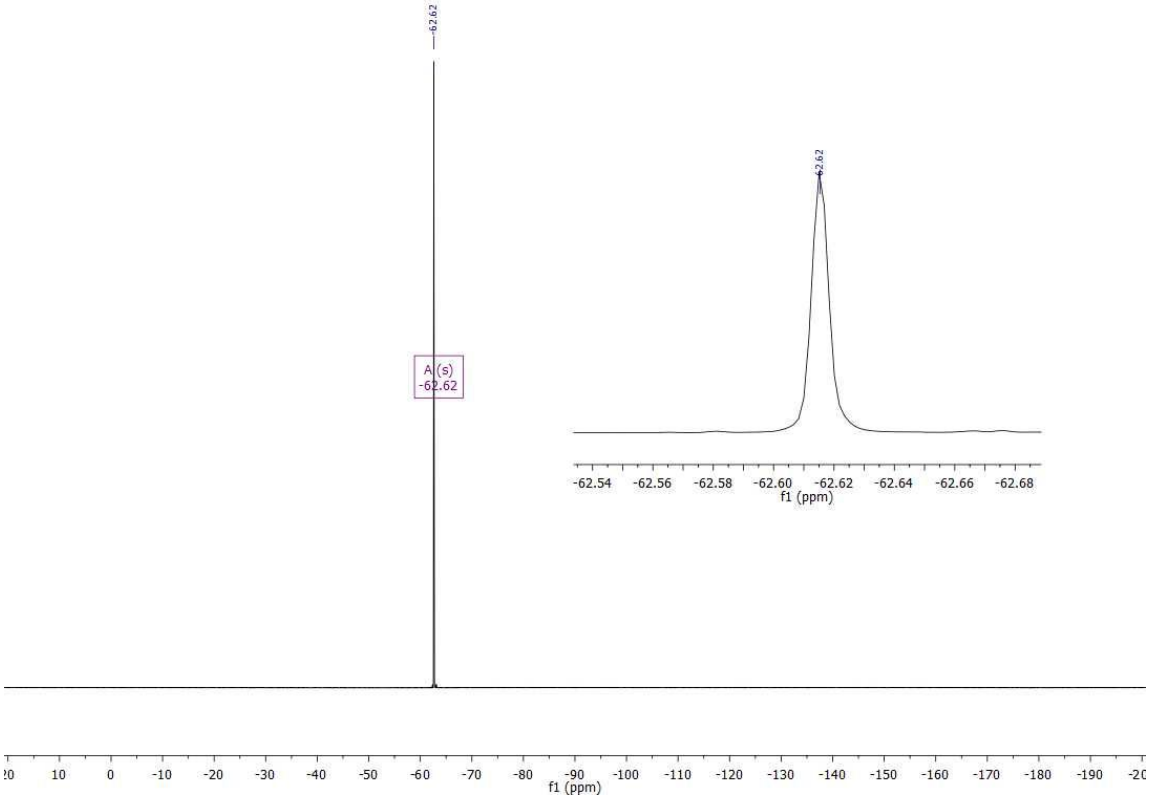
-62.62
A (s) -62.62
f1 (ppm)

REFERENCES

(1) Hirota, T.; Lewis, W. G.; Liu, A. C.; Lee, J. W.; Schultz, P. G.; Kay, S. A. A chemical biology approach reveals period shortening of the mammalian circadian clock by specific inhibition of GSK-3beta. *Proc. Natl. Acad. Sci.* **2008**, *105* (52), 5339.

(2) Yoo, S.-H.; Yamazaki, S.; Lowrey, P. L.; Shimomura, K.; Ko, C. H.; Buhr, E. D.; Siepka, S. M.; Hong, H.-K.; Oh, W. J.; Yoo, O. J.; Menaker, M.; Takahashi, J. S. PERIOD2::LUCIFERASE real-time reporting of circadian dynamics reveals persistent circadian oscillations in mouse peripheral tissues. *Proc. Natl. Acad. Sci.* **2004**, *101* (15), 5339.

(3) Kaneko, M.; Cahill, G. M. Light-Dependent Development of Circadian Gene Expression in Transgenic Zebrafish. *PLoS Biol.* **2005**, *3* (2), e34.

(4) McWilliam, H.; Li, W.; Uludag, M.; Squizzato, S.; Park, Y. M.; Buso, N.; Cowley, A. P.; Lopez, R. Analysis Tool Web Services from the EMBL-EBI. *Nucleic Acids Res.* **2013**, *41* (W1), 597.

(5) Li, W.; Cowley, A.; Uludag, M.; Gur, T.; McWilliam, H.; Squizzato, S.; Park, Y. M.; Buso, N.; Lopez, R. The EMBL-EBI bioinformatics web and programmatic tools framework. *Nucleic Acids Res.* **2015**, *43* (W1), 580.

(6) Sievers, F.; Wilm, A.; Dineen, D.; Gibson, T. J.; Karplus, K.; Li, W.; Lopez, R.; McWilliam, H.; Remmert, M.; Soding, J.; Thompson, J. D.; Higgins, D. G. Fast, scalable generation of high-quality protein multiple sequence alignments using Clustal Omega. *Mol. Syst. Biol.* **2014**, *7* (1), 539.

(7) Petzold, G.; Fischer, E. S.; Thomä, N. H. Structural basis of lenalidomide-induced CK1α degradation by the CRL4(CRBN) ubiquitin ligase. *Nature* **2016**, *532* (7597), 127.

(8) Mente, S.; Arnold, E.; Butler, T.; Chakrapani, S.; Chandrasekaran, R.; Cherry, K.; DiRico, K.; Doran, A.; Fisher, K.; Galatsis, P.; Green, M.; Hayward, M.; Humphrey, J.; Knafels, J.; Li, J.; Liu, S.; Marconi, M.; McDonald, S.; Ohren, J.; Paradis, V.; Sneed, B.; Walton, K.; Wager, T. Ligand-protein interactions of selective casein kinase 1δ inhibitors. *J. Med. Chem.* **2013**, *56* (17), 6819.

(9) Bischof, J.; Leban, J.; Zaja, M.; Grothey, A.; Radunsky, B.; Othersen, O.; Strobl, S.; Vitt, D.; Knippschild, U. 2-Benzamido-N-(1H-benzo[d]imidazol-2-yl)thiazole-4-carboxamide derivatives as potent inhibitors of CK1δ/ε. *Amino Acids* **2012**, *43* (4), 1577.

(10) Harder, E.; Damm, W.; Maple, J.; Wu, C.; Reboul, M.; Xiang, J. Y.; Wang, L.; Lupyan, D.; Dahlgren, M. K.; Knight, J. L.; Kaus, J. W.; Cerutti, D. S.; Krilov, G.; Jorgensen, W. L.; Abel, R.; Friesner, R. A. OPLS3: A Force Field Providing Broad Coverage of Drug-like Small Molecules and Proteins. *J. Chem. Theory Comput.* **2016**, *12* (1), 281.

(11) Friesner, R. A.; Banks, J. L.; Murphy, R. B.; Halgren, T. A.; Klicic, J. J.; Mainz, D. T.; Repasky, M. P.; Knoll, E. H.; Shelley, M.; Perry, J. K.; Shaw, D. E.; Perry Francis, A.; Shenkin, P. S. Glide: a new approach for rapid, accurate docking and scoring. 1. Method and assessment of docking accuracy. *J. Med. Chem*. **2004**, *47* (7), 1739.

(12) Friesner, R. A.; Murphy, R. B.; Repasky, M. P.; Frye, L. L.; Greenwood, J. R.; Halgren, T. A.; Paul C. Sanschagrin, A.; Mainz, D. T. Molecular Docking Studies of Alpinia galanga

Phytoconstituents for Psychostimulant Activity. *J. Med. Chem*. **2006**, *49*, 6177.

(13) Halgren, T. A.; Murphy, R. B.; Friesner, R. A.; Beard, H. S.; Frye, L. L.; W. Thomas Pollard, A.; Banks, J. L. Glide: a new approach for rapid, accurate docking and scoring. 2. Enrichment factors in database screening. *J. Med. Chem*. **2004**, *47* (7), 1750.

(14) Seabold, S.; Perktold, J. *Statsmodels: Econometric and Statistical Modeling with Python*; **2010**.

(15) Kuhn H. J.; Braslavsky S. E.; Schmidt R. Chemical actinometry (IUPAC Technical Report). *Pure Appl. Chem.*, **2004**, *76* (12), 2105.

(16) Hirota, T.; Lee, J. W.; Lewis, W. G.; Zhang, E. E.; Breton, G.; Liu, X.; Garcia, M.; Peters, E. C.; Etchegaray, J.-P.; Traver, D.; Schultz, P. G.; Kay, S. A. High-throughput chemical screen identifies a novel potent modulator of cellular circadian rhythms and reveals CKIα as a clock regulatory kinase. *PLoS Biol.* **2010**, *8* (12), e1000559.

(17) Oshima, T.; Niwa, Y.; Kuwata, K.; Srivastava, A.; Hyoda, T.; Tsuchiya, Y.; Kumagai, M.; Tsuyuguchi, M.; Tamaru, T.; Sugiyama, A.; Ono, N.; Zolboot, N.; Aikawa, Y.; Oishi, S.; Nonami, A.; Arai, F.; Hagihara, S.; Yamaguchi, J.; Tama, F.; Kunisaki, Y.; Yagita, K.; Ikeda, M.; Kinoshita, T.; Kay, S. A.; Itami, K.; Hirota, T. Cell-based screen identifies a new potent and highly selective CK2 inhibitor for modulation of circadian rhythms and cancer cell growth. *Sci. Adv.* **2019**, *5* (1), eaau9060.

(18) Ono, D., Honma, S., and Honma, K. Cryptochromes are critical for the development of coherent circadian rhythms in the mouse suprachiasmatic nucleus. *Nat. Commun.* **2013,** *4*, 1666.

(19) Zielinski, T.; Moore, A. M.; Troup, E.; Halliday, K. J.; Millar, A. J. Strengths and limitations of period estimation methods for circadian data. *PLoS One* **2014**, *9* (5), e96462.